Eur. Phys. J. C (2024) 84:694
https://doi.org/10.1140/epjc/s10052-024-13039-3

THE EUROPEAN PHYSICAL JOURNAL C

Regular Article - Theoretical Physics

Charged and magnetized particle motion around a static black hole in the Starobinsky–Bel–Robinson gravity

Akbar Davlataliev[1,2,a], **Bakhtiyor Narzilloev**[1,2,3,b], **Ibrar Hussain**[4,c], **Ahmadjon Abdujabbarov**[2,5,d], **Bobomurat Ahmedov**[2,3,5,e]

[1] New Uzbekistan University, Mustaqillik avenue 54, Tashkent 100000, Uzbekistan
[2] Ulugh Beg Astronomical Institute, Astronomy St. 33, Tashkent 100052, Uzbekistan
[3] Institute of Fundamental and Applied Research, National Research University TIIAME, Kori Niyoziy 39, Tashkent 100000, Uzbekistan
[4] School of Electrical Engineering and Computer Science, National University of Sciences and Technology, H-12, Islamabad, Pakistan
[5] University of Tashkent for Applied Sciences, Str. Gavhar 1, Tashkent 100149, Uzbekistan

Received: 16 April 2024 / Accepted: 24 June 2024

Abstract In this work we focus on the effects of Starobinsky–Bel–Robinson (SBR) gravity parameter and external magnetic field on the motion of charged test particles and magnetic dipoles moving around a black hole in the selected gravity theory. We take the external magnetic field to be uniform and aligned along the axis of symmetry. Our results reveal that the effect of the SBR gravity parameter is very strong in the close environment of the central black hole while in the farther distances this effects diminishes very quickly. We see that the effect of the external magnetic field on the particle motion is always dominating over the SBR gravity parameter in farther distances. We show that for the motion of charged test particles the magnetic interaction can mimic the spin up to very rapid rotations for prograde motion of particles, while for the motion of magnetic dipoles magnetic interaction can mimic the spin completely for retrograde motion of such particles. We observe that in both scenarios, the SBR gravity parameter behaves as a weak mimicker of the spin of Kerr black hole. We apply the outcomes of our study to the scenario where a neutron star is assumed to behave as a magnetic dipole moving around the supermassive black hole Sgr $A^\star$ to investigate how the magnetic field and the SBR gravity coupling parameter β affect the orbits of neutron stars orbiting the supermassive black hole.

1 Introduction

One of the most intriguing objects in astrophysics are black holes (BHs). The astrophysical processes around BH are mostly described by the general relativity (GR). GR has been successfully tested in both weak (using, e.g. solar system tests [1,2]) and strong field regimes (using gravitational wave observation [3] and observation of shadow of BHs [4]). However, current resolution of these experiments/observations leaves open windows for testing modified or alternative theories of gravity. One needs some modifications and alternatives to the GR in order to resolve some fundamental issues (singularity, non-compatibility with quantum field theory, problems related to nature of dark energy/matter) with this theory of gravity. One of the modifications of GR is known as the the SBR model. The SBR model involves modification due to the addition of quadratic terms, incorporating the Bel–Robinson tensor and the Ricci scalar, within the Einstein–Hilbert action [5,6]. The SBR modified gravity theory is associated with the low-energy eleven-dimensional string theory or M-theory. This theory is distinguished by a dimensionless coupling parameter, $\beta > 0$, which can be determined through the compactification process of the M-theory [7]. The parameters of the SBR theory of gravity makes this theory applicable in the BH Physics and inflationary Cosmology [6].

The structure of the electromagnetic field around compact objects plays very important role in astrophysics. Strong gravity through the spacetime curvature affects the electromagnetic field. One needs to take into account the effects of gravity while considering the effect of magnetic field on radiation mechanisms of neutron stars [8,9]. On the other

[a] e-mail: akbar@astrin.uz
[b] e-mail: baxtiyor@astrin.uz
[c] e-mail: ibrar.hussain@seecs.nust.edu.pk (corresponding author)
[d] e-mail: ahmadjon@astrin.uz
[e] e-mail: ahmedov@astrin.uz

Published online: 14 July 2024

hand, during the collapse the proper magnetic momentum of the star will decay with the time and at the final stage BH will not have own magnetic field [10]. No-hair theorem also claims that BH may not have own magnetic field [11]. However, astrophysical BH may be surrounded by external electromagnetic field caused by the companion star or accretion disc containing electric current [12]. It was R. Wald who first obtained the solution of Maxwell equation around rotating BH immersed in external asymptotically uniform magnetic field. This toy model qualitatively describes the electromagnetic field structure change due to spacetime structure.

Test particle motion may play a role of probe of metric theories of gravity. On the other hand the charged and magnetized particle dynamics maybe used to test both electromagnetic and curvature structure surrounding BHs. A big number of works have been devoted to study the dynamics of charged and magnetized particles around compact object in different gravity models [13–30]. Particularly, the circular orbits provides more information about the central object [31]. Innermost stable circular orbits (ISCO) of the particles around BHs is one of the main features of the GR. The inner edge of the accretion disc around BHs are associated with ISCO. Thus ISCO may provide a useful tool to compare the theoretical results and the observations in order to get parameter estimation/constraint [32]. We would like to highlight that our prior research has thoroughly examined the characteristics of diverse BH solutions, employing various approaches as detailed in [33–46].

In this paper we study the dynamics of the charged and magnetized particles around a BH described in the SBR gravity. The paper is organized as follows. We start with the review of the spherically symmetric and static BH solution in the SBR gravity in Sect. 2. The Sect. 3 is devoted to the analysis of the charged particle motion in the vicinity of the BH in the SBR theory of gravity. The magnetized particles dynamics around the static BH in the SBR gravity are explored in Sect. 4. We consider some astrophysical applications of the obtained results in Sect. 5. Finally, we conclude our results in Sect. 6.

2 Schwarzschild-type black hole in the Starobinsky–Bel–Robinson gravity

In this section we revisit the spacetime structure of the static and spherically symmetric BH solution within the context of the SBR gravity, which is embedded in the M-theory existing in an eleven-dimensional spacetime [47]. The M-theory is on a bosonic sector is a string theory that incorporates a metric and a tensor 3-form CMND, which are coupled to M2-branes and dual to M5-branes [48]. By employing the compactification mechanism along with the inclusion of stringy fluxes, required for the stabilization scenarios, one can derive corresponding four-dimensional gravity models [7,47]. In simpler terms, the action of the SBR theory of gravity can be expressed as follows:

$$S_{SBR}=\frac{M_{pl}^2}{2}\int d^4x\sqrt{-g}\left[R+\frac{R^2}{6\mu^2}-\frac{\beta}{32M_{pl}^6}(\mathcal{P}^2-\mathcal{G}^2)\right]. \tag{1}$$

In the last equation, g represents the determinant of the metric tensor, M_{pl} denotes the reduced Planck mass, which can be approximated as $M_{pl}=1/\sqrt{8\pi G}\approx 2\times 10^{18}$GeV, and R represents the Ricci scalar curvature. The free mass parameter μ can have various interpretations depending on the nature of the specific theory being studied. The quadratic contributions $\mathcal{P}^2$ and $\mathcal{G}^2$ are associated with the Pontryagin and Euler topological densities, respectively. The final term is connected to the Bel–Robinson tensor, as explained in references [7,47].

$$T^{\mu\nu\lambda\rho}T_{\mu\nu\lambda\rho}=\frac{1}{4}(\mathcal{P}^2-\mathcal{G}^2) \tag{2}$$

where the new 4-rank tensor

$$T^{\mu\nu\lambda\sigma}=R^{\mu\rho\gamma\lambda}R^{\nu\sigma}_{\rho\gamma}+R^{\mu\rho\gamma\sigma}R^{\nu\lambda}_{\rho\gamma}-\frac{1}{2}g^{\mu\nu}R^{\rho\gamma\alpha\lambda}R^{\sigma}_{\rho\gamma\alpha} \tag{3}$$

is introduced.

The action of the SBR gravity introduces two additional parameters, μ and β, compared to the Hilbert action in GR. This modification has been utilized to obtain novel physical models, such as inflationary model of Cosmology. In the context of the SBR gravity, static Schwarzschild-like BH solution was derived, and the parameter μ was determined by solving the equation of motion [7]. It was shown that the thermodynamic properties of this static BH are affected by the stringy gravity parameter β. Consequently, the line element of this Schwarzschild-like solution can be expressed as follows:

$$ds^2=-f(r)dt^2+\frac{1}{f(r)}dr^2+r^2d\Omega^2 \tag{4}$$

where the metric function $f(r)$ is

$$f(r)=1-\frac{r_s}{r}+\beta\frac{128M^6\pi^3}{5}\left(\frac{r_s}{r^3}\right)^3\left(108-97\frac{r_s}{r}\right). \tag{5}$$

Additionally, we have $r_s=2M$, where M represents the total mass parameter of the BH.

3 Charged particle motion

3.1 Magnetic field around compact object

By utilizing the Wald method [12], it is possible to identify the elements of the four-vector potential that align with the

magnetic field, in the following manner:

$$A^{\mu} = \left(0, 0, 0, \frac{1}{2}B\right). \tag{6}$$

With the metric (4) at hand, it is possible to express the covariant components as

$$A_{\mu} = \left(0, 0, 0, \frac{1}{2}Bg_{\phi\phi}\right). \tag{7}$$

One can now derive the expression for the magnetic field surrounding a compact object. The four-velocity of the proper observer is provided by

$$\mathcal{U}^{\alpha} = \left\{1/\sqrt{-g_{tt}}, 0, 0, 0\right\}. \tag{8}$$

Subsequently, the orthonormal components of the magnetic field, with respect to the selected frame, can be expressed as follows [49].

$$B^{\hat{r}} = B\cos\theta \; B^{\hat{\theta}} = B\sqrt{f}\sin\theta. \tag{9}$$

In the limit of the Newtonian weak field regime, where $M/r \to 0$, the components of the magnetic field transform into

$$B^{\hat{r}} = B\cos\theta \; B^{\hat{\theta}} = B\sin\theta \tag{10}$$

which is consistent with the Newtonian limit.

3.2 Circular motion of charged test particle around a BH in the SBR theory of gravity

Here, we briefly examine the equation of motion governing a charged particle orbiting the compact object in the SBR gravity. It is advantageous to employ the Hamilton-Jacobi equation for particle motion around central objects, as is the situation here. When an external electromagnetic field is present, this equation takes the form:

$$g^{\alpha\beta}\left(\frac{\partial S}{\partial x^{\alpha}} + eA_{\alpha}\right)\left(\frac{\partial S}{\partial x^{\beta}} + eA_{\beta}\right) = -m^2, \tag{11}$$

where e and m denote the electric charge and mass of the test particle, respectively. Equation (11) does not exhibit separability in non-integrable systems. In such instances, Equation (11) is substituted with a Hamiltonian formalism [50–55]. Nonetheless, when exploring test particle motion in the equatorial plane, Eq. (11) can be rephrased in the following separable form:

$$S = -Et + L\phi + S_r + S_{\theta}. \tag{12}$$

Here, E and L represent the energy and angular momentum of a test particle, respectively. Therefore, the equation of motion for a unit mass test particle is given by

$$\frac{\mathcal{E}^2}{g_{tt}} + \frac{1}{g_{rr}}\left(\frac{\partial S}{\partial r}\right)^2 + \frac{1}{g_{\phi\phi}}\left(\mathcal{L} + \frac{e}{m}A_{\phi}\right)^2 = -1. \tag{13}$$

Here, $\mathcal{E} = E/m$ and $\mathcal{L} = L/m$ represent the specific energy and angular momentum of a test particle, respectively.

For test particles moving in the equatorial plane ($\theta = \pi/2$), the radial motion

$$-\frac{g^{rr}}{g^{tt}}\dot{r}^2 = (\mathcal{E} - \mathcal{V}_{eff})(\mathcal{E} + \mathcal{V}_{eff}) \tag{14}$$

can be used to determine the effective potential which reads

$$\mathcal{V}_{eff} = \sqrt{-g_{tt}\left(\frac{(L - \omega_B g_{\phi\phi})^2}{g_{\phi\phi}} + 1\right)}, \tag{15}$$

where $\omega_B = -eB/(2mc)$ denotes the charged particle's cyclotron frequency, which is related to the interaction of the charged particle with the external magnetic field. Figure 1 illustrates the radial dependence of such an effective potential. Left panel illustrates that increase of the parameter β strengthens the effective potential considerably for the fixed angular momentum and particle's cyclotron frequency. The right panel however, shows that the effect of the magnetic field is not monotonic everywhere. We see that in the presence of the parameter β magnetic field effects changes with the distance between the central compact object and the test particle. For bigger distance one can see that lines are going up monotonically. This is due to the chosen model where we assume that the entire space is filled with uniform magnetic field whose Lorentz force becomes stronger compared to the gravitational attraction at far distances. Since we are primarily interested in the vicinity of BHs, this does not significantly affect the phenomena we are focused on.

The following standard conditions can be established for a particle moving in a circular orbit in the equatorial plane:

$$\mathcal{V}_{eff} = \mathcal{E}, \mathcal{V}'_{eff} = 0 \tag{16}$$

which causes a charged test particle's angular momentum to have the radial dependence, shown in Fig. 2. In the spacetime described by Eq. (4), the parameter β has a repulsive effect. For non-zero values of β, the ISCOs are expected to decrease for a given angular momentum. As the radial coordinate decreases, the repulsive force due to the parameter β becomes more significant. Consequently, particles can maintain circular orbits with smaller angular momentum. When the repulsive force surpasses the attractive force, the angular momentum becomes zero. Below this critical distance, circular orbits for particles are not possible. It can be demonstrated that negative values of angular momentum, indicating motion in the opposite direction, have a dependence on the radial coordinate that is symmetric with respect to the r-axis on the graph shown in the Fig. 2

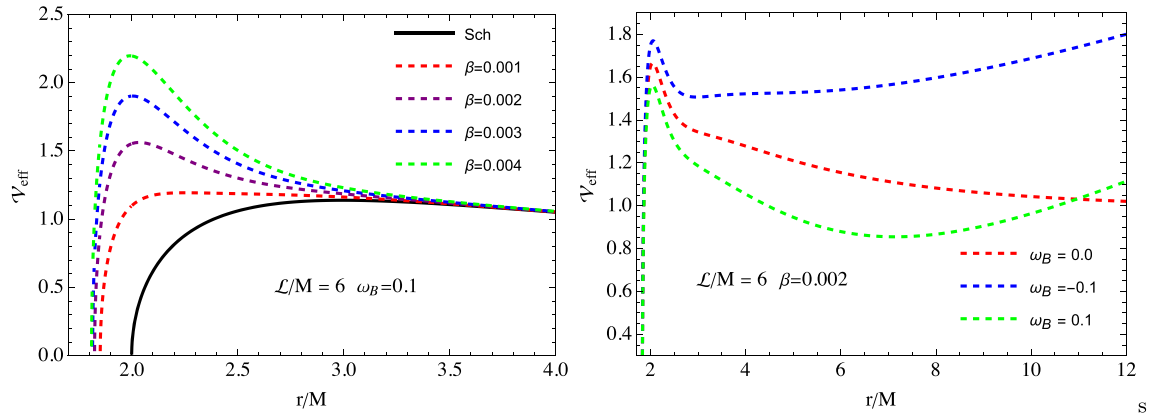

Fig. 1 Radial dependence of the effective potential on the different values of the magnetic interaction (right panel) and parameter β (left panel)

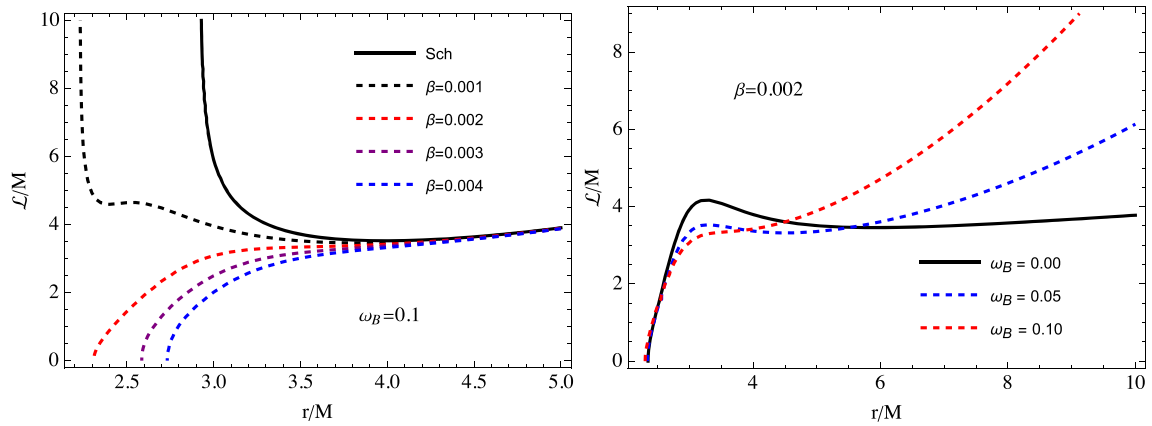

Fig. 2 Angular momentum as a function of radial coordinate r. The left panel corresponds to the variation of the β parameter. The right panel is for the variation of the magnetic interaction

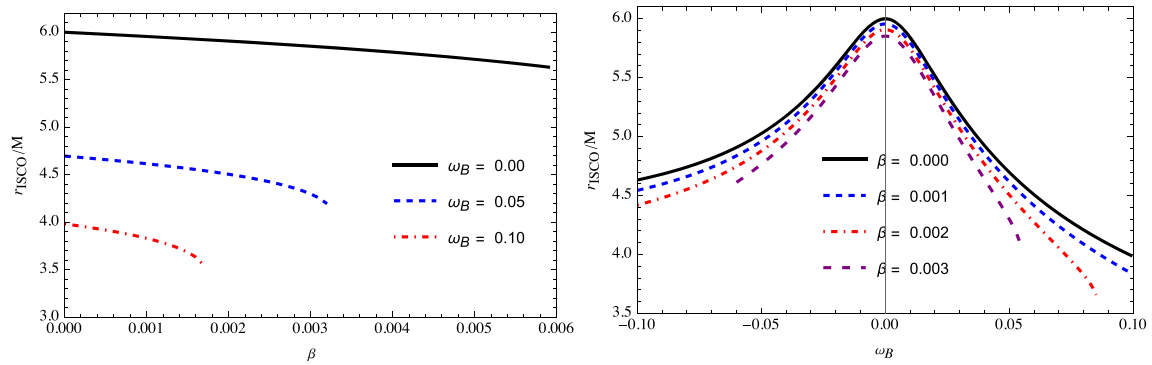

Fig. 3 ISCO radius of a test particle orbiting in the equatorial plane of the SBR compact object for different values of the magnetic interaction (right panel) and β parameter (left panel)

3.3 Innermost stable circular orbits

We study the ISCO around a compact object in the SBR gravity submerged in an asymptotically uniform magnetic field in this subsection. We attempt to provide an answer to the question of how the parameters β and ω_B can resemble the rotation parameter a of the well-known Kerr solution, based on the results obtained. The objective is to establish a constrained relationship between the rotation parameter and the parameters β and ω_B for a given ISCO radius, provided that the mentioned parameters can simulate the rotation parameter of the Kerr BH. Initially, we look into the relationship between the parameters of interest and the ISCO radius. In order to accomplish this, one can amend the conditions (16),

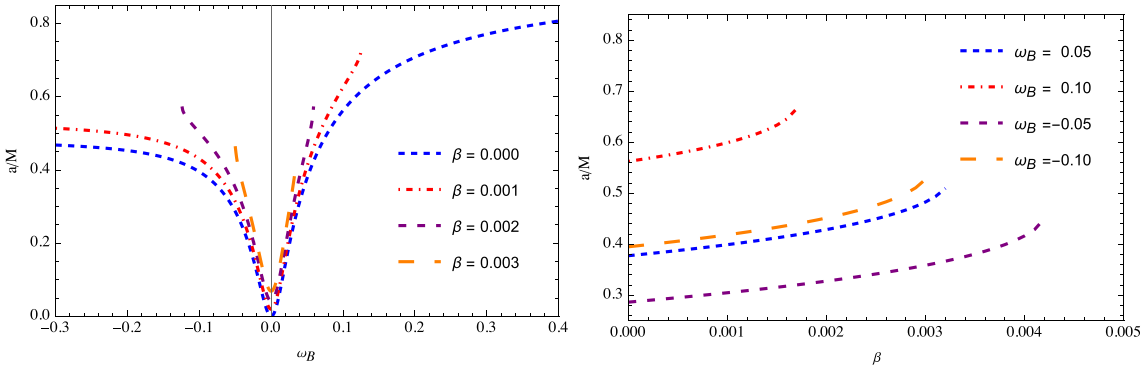

Fig. 4 Degeneracy plot that shows the correspondence between the rotation parameter a of the Kerr metric, and ω_B and β parameters

reading

$$\mathcal{V}''_{eff} = 0 \tag{17}$$

By considering these three conditions (along with Eq. (16)), it is possible to visualize the interdependence between the ISCO radius and the parameters β and ω_B as illustrated in Fig. 3. The plotted graphs clearly demonstrate that increasing the values of both β and ω_B leads to a reduction in the ISCO radius experienced by a charged test particle. It is evident from the left panel that as the β parameter is increased to a certain value, the ISCO radius goes down monotonically up to specific value depending on the value of the external magnetic field. From the right panel one can see that ISCO radius has a maximum value in the absence of the external magnetic field. One can also notice that for bigger values of the spacetime parameter β the length of the lines becomes shorter suggesting that existence of the ISCOs is restricted by this parameter.

Ultimately, our goal is to address the initial question posed at the start of this subsection: to what extent can the parameters β and ω_B emulate the rotation parameter a of the Kerr metric for the matching ISCO radii? By understanding how the ISCO behaves in the presence of the rotation parameter in the case of the Kerr metric, one can visualize the relationship between these parameters, depicted in Fig. 4. In the left panel the degeneracy lines for a and ω_B are shown, when β takes fixed values. In the right panel, it is evident that β parameter itself (i.e in the absence of external magnetic field) can imitate the rotation parameter only up to approximately ≈ 0.2 in the absence of an external magnetic field. However, with the "help" of external magnetic field it is possible to mimic the spin of the pure Kerr BH up to bigger values of the spin parameter.

Figure 5 depicts the degeneracy, diagram is showing the relationship between the parameter β and the magnetic coupling parameter ω_B for several predetermined ISCO radius values. It is apparent that the magnetic interaction exerts a significantly more pronounced influence compared to the effect of the spacetime parameter β.

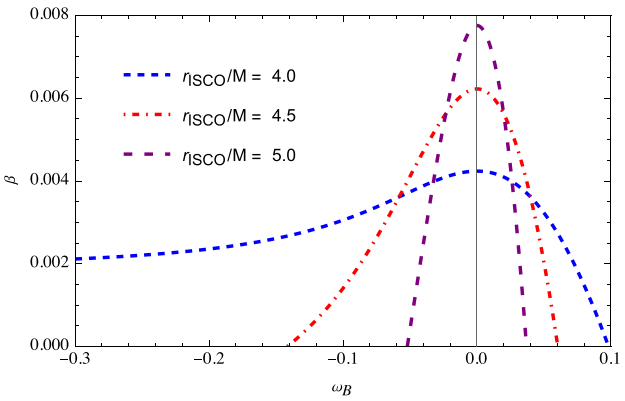

Fig. 5 Degeneracy plots for β and ω_B for given values of ISCO radii

The trajectories of orbits near the BH are shown in Fig. 6. In the top two panels we vary magnetic interaction parameter, keeping fix β, while in the bottom two we fix the magnetic interaction parameter and change the parameter β. In the plots, dashed lines show the boundary of trajectory of a particle in x-z plane. From the comparison of top two panels we can see that decrease of the magnetic interaction parameter reduces the boundary size in the z direction but increases in the x (radial) direction. When one compares the middle one with the third panel it can be seen that there is a negligible change in the boundary of the trajectories, but the shape of the trajectories experiences considerable change.

4 Magnetic dipole motion: The SBR gravity black hole versus the Kerr black hole

The motion of the magnetic dipole surrounding the SBR gravity compact object submerged in an asymptotically uniform magnetic field is the main topic of discussion in this section. The magnetic dipole's Hamilton-Jacobi equation of

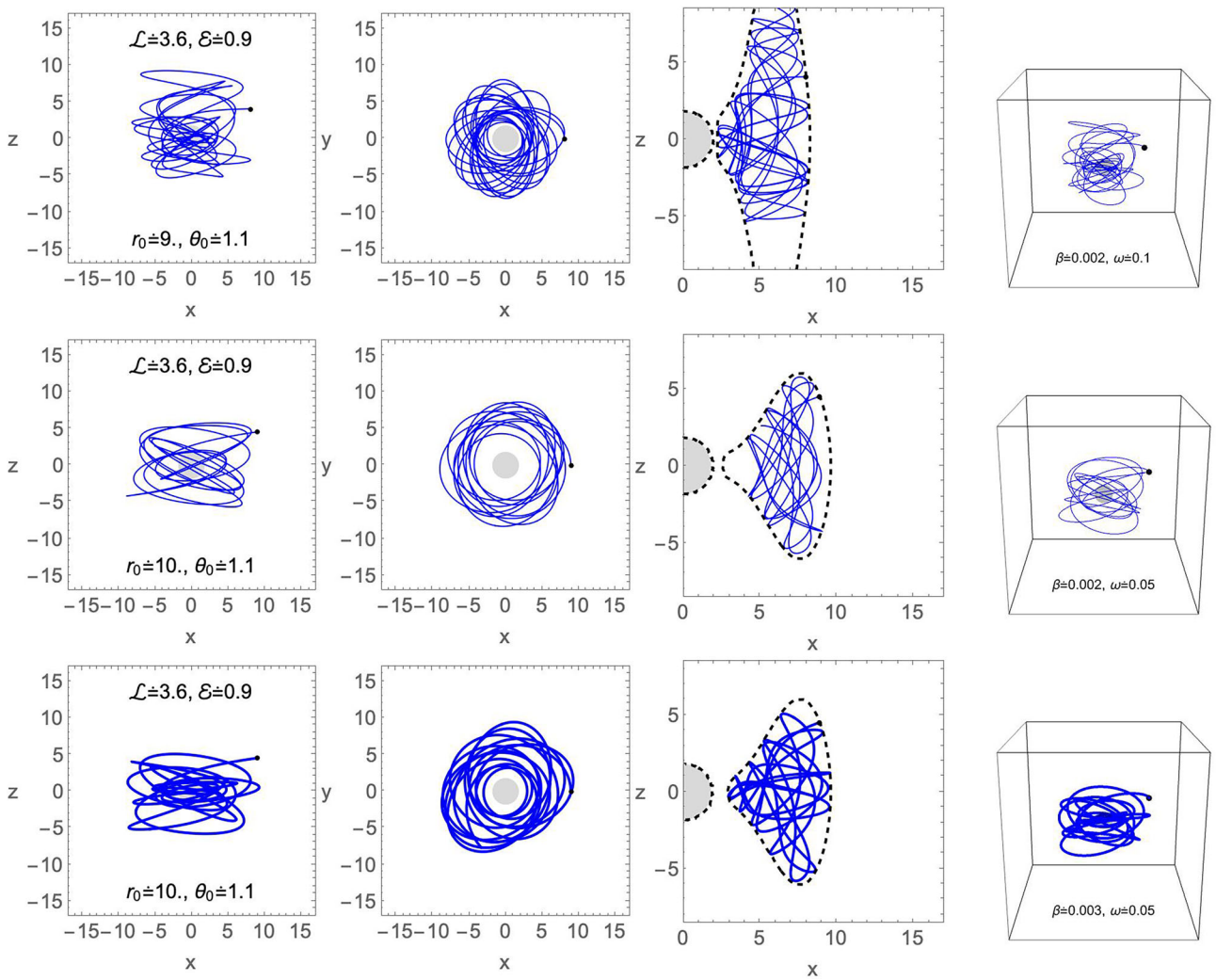

Fig. 6 Trajectories of test particles (depicted as solid curves) around the BH are illustrated within the confines of the shaded circle, excluding the consideration of external electric fields. The fourth column displays the 3D particle trajectories, while the first and second columns represent their 2D orientations. By employing the principles of energy and angular momentum conservation, we can represent the 4D configuration space (t, x, y, z) in a 2D graph (third column), where the motion boundary is delineated using the effective potential (dotted-dashed curves)

motion is as follows

$$g^{\mu\nu}\frac{\partial S}{\partial x^{\mu}}\frac{\partial S}{\partial x^{\nu}} = -\left(m - \frac{1}{2}D^{\mu\nu}F_{\mu\nu}\right)^2. \tag{18}$$

The antisymmetric polarization tensor, $D^{\mu\nu}$, in this case specifies the particle's electrodynamics characteristics. Here we assume that the particle is electrically neutral, $q = 0$, and that only the magnetic moment μ itself can describe the polarization tensor. It is important to note that the motion of the magnetic dipole with an electric charge can also be investigated in a different way by taking the left hand side of Eq. (11) rather than the one in Eq. (18). In this work, however, we want to apply the motion of the magnetic dipoles to magnetized neutron stars, which can be considered as electrically neutral test particles with nonvanishing magnetic dipole moment, orbiting around supermassive BHs. We can use a neutron star as a test particle traveling in the considered spacetime because the mass of a supermassive BH is significantly larger than the mass of a neutron star. Thus, from now on, we will only be concentrating on the motion of an electrically neutral magnetic dipole. The elements of this tensor in this instance can be expressed as [56].

$$D^{\mu\nu} = \eta^{\mu\nu\alpha\beta}u_{\alpha}\mu_{\beta}, \tag{19}$$

which satisfies the following condition:

$$D^{\mu\nu}u_{\nu} = 0, \tag{20}$$

where the magnetic dipole's four-momentum is described by μ_{α}, $F_{\mu\nu}$=$\partial_{\mu}A_{\nu}$-$\partial_{\nu}A_{\mu}$ is electromagnetic field tensor which is also expressed in terms of the electromagnetic field's con-

stituent parts as

$$F_{\mu\nu} = -\eta_{\mu\nu\alpha\beta} B^{\alpha} u^{\beta} + 2[u_{\mu} E_{\nu}]. \tag{21}$$

Here the Levi–Civita symbol $\epsilon_{\alpha\beta\sigma\gamma}$ is defined as follows: $\eta_{\alpha\beta\sigma\gamma}$ is the pseudo-tensorial form of this symbol.

$$\eta_{\alpha\beta\sigma\gamma} = \sqrt{-g}\epsilon_{\alpha\beta\sigma\gamma}, \quad \eta^{\alpha\beta\sigma\gamma} = \frac{1}{\sqrt{-g}}\epsilon^{\alpha\beta\sigma\gamma} \tag{22}$$

With the spacetime metric (4) g=det$|g_{\mu\nu}|= -r^4 \sin^2\theta$ and

$$\epsilon_{\alpha\beta\sigma\gamma} = \begin{cases} +1, & \text{for even permutations} \\ -1, & \text{for odd permutations} \\ 0, & \text{for the other combinations} \end{cases} \tag{23}$$

After utilizing (19) for the contraction and (20) for (21), one can write

$$D^{\mu\nu} F_{\mu\nu} = 2\mu^{\alpha} B_{\alpha} = 2\mu^{\hat{\alpha}} B_{\hat{\alpha}} \tag{24}$$

Because of the external test magnetic field's weakness, we will consider the magnetic interaction between the magnetic dipole and the external magnetic field to be sufficiently weak for the sake of simplicity. Consequently, we can use the approximation $(\mathcal{D}^{\mu\nu}\mathcal{F}_{\mu\nu})^2 \to 0$. It is anticipated that a particle's magnetic momentum will align with an external magnetic field in a given situation. Assuming a particle moving at the equatorial plane ($\theta = \pi/2$), the magnetic moment $\mu^{\hat{\theta}}$ is consistent with the lowest energy condition of the magnetic dipole, since this magnetic field has only a normal component $B^{\hat{\theta}}$ to this equatorial plane. Then, the scalar product (24) is

$$D^{\mu\nu} F_{\mu\nu} = 2\mu B\mathcal{A} \tag{25}$$

Here, considering Eq. (9), $\mathcal{A}(r)$ defines the proportionality function, and for $B^{\hat{\theta}}$, reads

$$\mathcal{A} = f(r)(f(r) - \Omega^2 r^2)^{-\frac{1}{2}} \tag{26}$$

By inputting the scalar product of $D^{\mu\nu}$ and $F^{\mu\nu}$ into Eq. (18) of motion, the effective potential at the equatorial plane can be determined as

$$\mathcal{V}_{eff} = \sqrt{\frac{1 - \alpha\mathcal{A} + g^{\phi\phi}\mathcal{L}^2}{-g^{tt}}} \tag{27}$$

where $\alpha = 2\mu B/m$.

The electromagnetic interaction between a magnetic dipole and an external magnetic field is defined by the magnetic coupling parameter, α. When a normal neutron star with a magnetic dipole moment of $\mu = (1/2)B_{NS}R_{NS}^3$ circles a supermassive BH for instance, in real astrophysical scenarios, the coupling magnetic parameter is

$$\alpha \simeq \frac{11}{250}\left(\frac{B_{NS}}{10^{12}G}\right)\left(\frac{R_{NS}}{10^6 cm}\right)^3\left(\frac{B_{ext}}{10G}\right)\left(\frac{m_{NS}}{M_{\odot}}\right)^{-1} \tag{28}$$

where R_{NS} and m_{NS} stand for the neutron star's mass and radius, respectively, and B_{NS} is the magnetic field at the star's surface. Figure 7 shows a plot of the effective potential's radial dependence. We observe that the magnetic dipole's effective potential behaves similarly to that of the charged particle in relatively closer orbits but for relatively far distances one can notice the difference.

By using the same conditions (16) for the particle's trajectory to be circular, one can readily derive the equations for the angular momentum and the energy of the test particle.

When a particle's orbit at the equatorial plane is circular, the radial dependence of the particle's angular momentum is illustrated in Fig. 8. One can again see the similarity of the behavior of the lines with the electrically charged test particle in the close distances from the central BH. However, once again, they behave differently at far distances.

After acquiring the effective potential and the radial variation for the angular momentum, one can proceed to examine the ISCO for a magnetic dipole in motion at the equatorial plane. We can utilize either the condition specified in Eq. (17) or the angular momentum to ensure a minimum at the ISCO radius. Consequently, the representation of the ISCO radius in terms of the parameter β and the magnetic coupling parameter α is depicted in Fig. 9. The right panel shows the impact of β for several values of α, while the left panel illustrates the effect of the magnetic coupling parameter for different values of the parameter β. The left plot reveals that as the magnetic coupling parameter increases, the ISCO radius also increases especially, at around $\alpha = 0.3$ it goes up exponentially. From the right panel it can be seen that the effect of the parameter β on the ISCO radius is very weak as compared with the magnetic coupling parameter.

5 Astrophysical applications of the study

A critical and relevant concern within relativistic astrophysics involves examining the theory of gravity through the study of the motion of test magnetic dipoles, particularly in relation to the movement of neutron stars (pulsars and/or magnetars) treated as test magnetic dipoles around supermassive BHs. This exploration offers an opportunity to probe both gravitational and electromagnetic fields around a supermassive BH, as their precise pulses in observations can aid in measuring distance through the Doppler effect. Through observations of such scenarios, it becomes evident that a neutron star may be situated near a galactic center. At present, the task of locating radio pulsars is notably challenging due to the Compton scattering of radio pulses within a densely charged electron gas encircling the Sgr $A^{\star}$. The discovery of the first and so far the only neutron star-magnetar, named SGR 1745-2900, around Sgr $A^{\star}$ occurred in 2013 [57]. In our calculations, we utilize the parameters of the

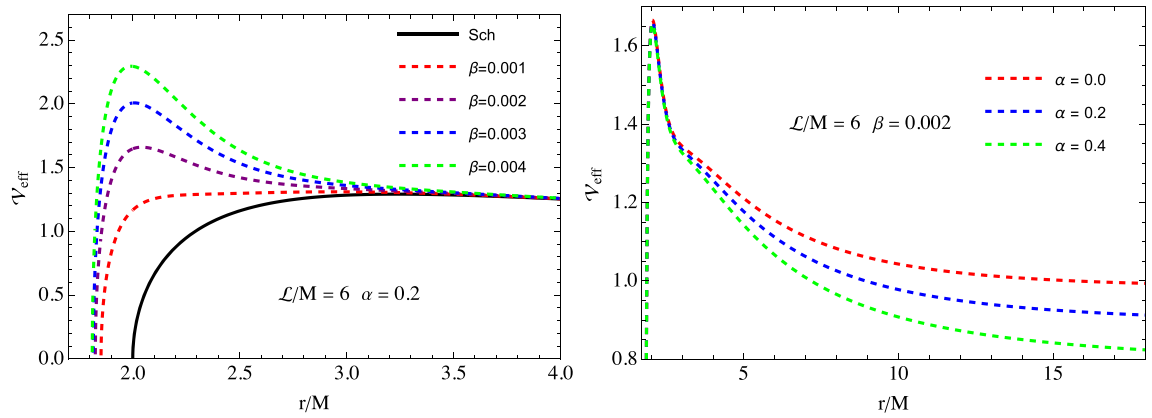

Fig. 7 Effective potential for various values of the β (left panel) and magnetic interaction (right panel), as a function of r/M

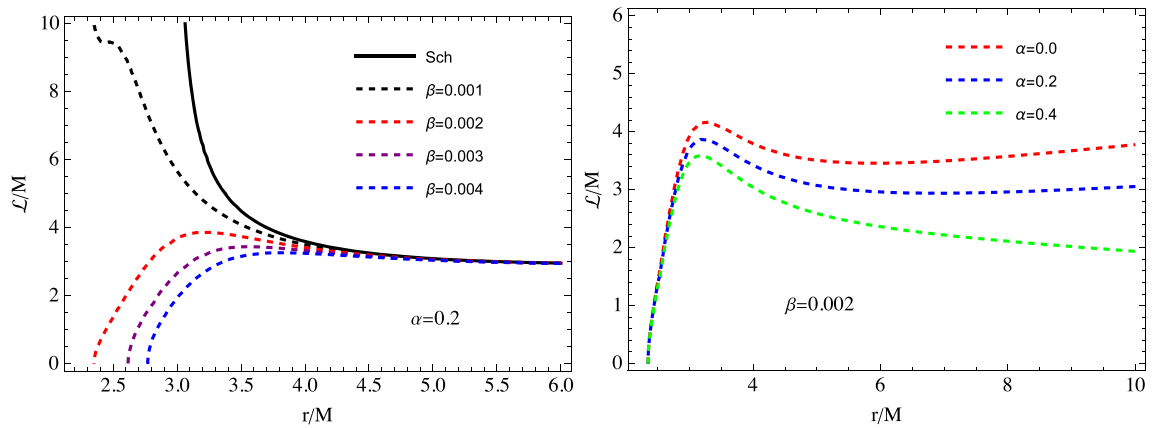

Fig. 8 Dependence of a magnetic dipole's angular momentum radially on various values of the magnetic parameter α (right panel) and parameter β (left panel)

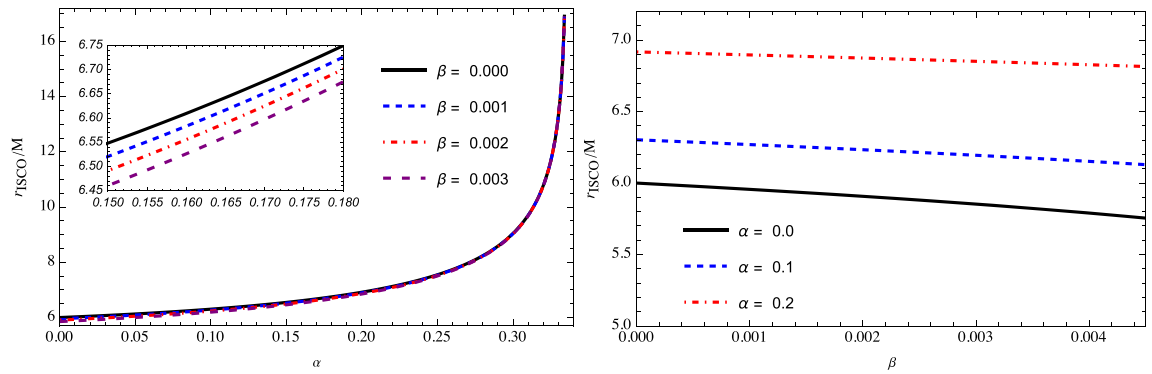

Fig. 9 Dependency between test particle ISCO radius and parameter β for a given α (right panel) and magnetic coupling parameters for a given β (right panel) around the SBR gravity BH orbiting at the equatorial plane

magnetar, treating it as a magnetic dipole in orbit around Sgr $A^{\star}$. Conversely, theoretical challenges arise in the analysis of observational traits, such as quasi periodic oscillations and the ISCO radius around the supermassive BH, when similar effects on these properties are reflected by the parameters of different alternative theories of gravity, making it difficult for gravity's influence to be predominant. In fact, rotating BHs are predominantly accepted in astrophysics. Our aim is to examine the ISCO radius, comparing it with the effects of spacetime and the spin of the Kerr BH, when both yield identical ISCO radius values for the magnetic dipoles. It is important to note that for comparison, we consider the SBR gravity compact object surrounded by an externally asymptotically uniform magnetic field and the Kerr BH without a

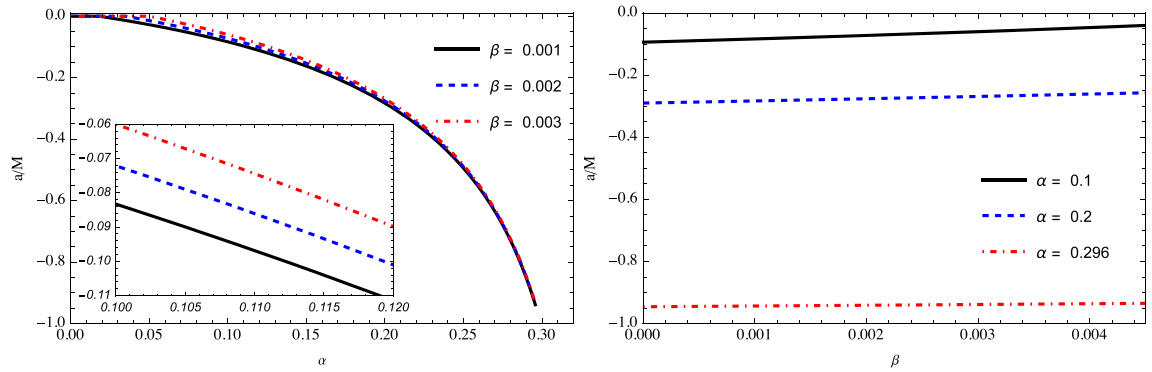

Fig. 10 A degeneracy plot is depicted, showing the relationship between the dimensionless spin of the Kerr BH and the magnetic coupling parameter α and the parameter β

magnetic field. We assume the actual astrophysical scenario of the magnetar orbiting the supermassive BH Sgr $A^{\star}$. Additionally, one may consider a magnetic dipole as a neutral one in the absence of an external magnetic field.

The magnetic coupling parameter α for the magnetar SGR (PSR) J1745-2900, characterized by the magnetic dipole moment $\mu \simeq 1.6 \times 10^{32} G \cdot \mathrm{cm}^3$, while orbiting the supermassive BH Sgr $A^{\star}$, is [57].

$$\alpha_{\text{PSR J1745-2900}} \simeq 0.716 \left(\frac{B_{ext}}{10G}\right) \tag{29}$$

So, we see that one can take the coupling parameter in the order of $\alpha \sim 10^{-1}$ in real scenarios.

The ISCO radius of test particles circling the Kerr BH is determined by the subsequent expression for retrograde (+) and prograde (−) orbits [32]:

$$r_{\text{isco}} = 3 + Z_2 \pm \sqrt{(3 - Z_1)((3 + Z_1 + 2Z_2)}, \tag{30}$$

where

$$Z_1 - 1 = \left(\sqrt[3]{1+a} + \sqrt[3]{1-a}\right)\sqrt[3]{1-a^2},\ Z_2^2 - Z_1^2 = 3a^2. \tag{31}$$

In this discussion, our focus will be on how the magnetic coupling parameter can replicate the spin of the Kerr BH, yielding an equivalent value for the ISCO radius of the magnetic dipoles around the SBR gravity BH. It is straightforward to determine the ISCO radius for magnetic dipoles around the SBR gravity BH while maintaining the β parameter very small.

A degeneracy plot can be generated, correlating the magnetic parameter in our model with the rotation parameter of the Kerr metric. As depicted in the left panel of Fig. 9, it becomes evident that, when the β parameter is held constant, the ISCO radius grows in a manner similar to increasing the magnetic coupling parameter. This suggests that the coupling parameter is likely to imitate the rotation parameter of the Kerr metric for retrograde orbits. Figure 10 provides an illustration of this relationship, offering assurance on the matter. As can be seen from the left panel magnetic parameter can mimic the retrograde rotation of the Kerr BH completely. The right panel demonstrates the efficiency of the parameter β to mimic the spin of the Kerr BH is very low, suggesting that static BH in the SBR gravity without external magnetic field can not properly mimic rapidly rotating Kerr BH.

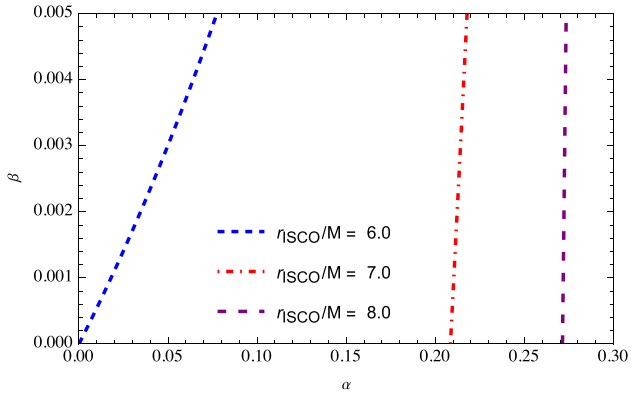

Fig. 11 Relationships between the magnetic coupling parameter α and the parameter β for constant ISCO radius values of the magnetic dipoles

Figure 11 displays the degeneracy relationship between the values of the parameter β and the magnetic coupling parameter for constant values of the ISCO radius. It is shown that for bigger ISCO radii the magnetic interaction plays the dominant role while for smaller orbits, β parameter becomes considerable.

6 Conclusion

This study focused on examining the motion of charged particles as well as magnetic dipoles around the Schwarzschild-like BH in the SBR gravity, aiming to assess the extent to which the spacetime deviation parameter and an external uniform magnetic field can imitate the rotation parameter of the Kerr BH.

When investigating the motion of a charged test particle, we found that the primary influence on the particle trajectories arises from the external magnetic field. The effect of the SBR gravity parameter β, on the other hand, is significant only in the immediate vicinity of the central BH. An increase in the β parameter was shown to enlarge the effective potential, contrasting with the impact of the external uniform magnetic field. Notably, the behavior of the latter changes with the radial coordinate of the test charged particle for positive ω_B. An exploration of circular motions through the angular momentum of the charged test particle revealed an absence of circular orbits in the close vicinity of the BH, when the value of β exceeds a specific threshold. In the spacetime given by (4) the effects of the parameter β has a repulsive nature. For the non vanishing values of the parameter β one may expect a decrease in the radius of the ISCOs for the given value of the angular momentum. With the decrease of radial coordinate the repulsive force due to the β parameter becomes significant. As a consequences the particles can stay on circular orbit with smaller angular momentum. At the point when repulsive force starts dominating over attractive one the angular momentum becomes zero and at a distance lower then this point the circular orbits of particles do not exist. One can show that the negative values of the angular momentum corresponds to motion in the opposite direction and its dependence on the radial coordinate is symmetric with respect to the r-axis on the graph in the Fig. 2.

Examining the dependence of the ISCO radius on the parameters β and ω_B, we observed that an increase in the β parameter reduces the ISCO radius, while an increase in absolute value of ω_B has a similar effect. We then compared the effects of β and ω_B with the effect of the spin of the Kerr BH for matching ISCO radii, establishing a degeneracy between the spin of the Kerr BH and the parameters of our model for the same ISCO radii. The results indicated that the β parameter can mimic the effect of the spin, but only up to small values, while ω_B performs this task more effectively, extending up to very rapid spins. Analyzing the trajectories of the charged test particle, we found that an increase in the magnetic interaction parameter widens the region of possible particle trajectories along the axis of symmetry while narrowing it in the radial direction. In contrast, an increase in the β parameter has a negligible effect in this regard but significantly alters the path of motion.

Subsequently, our focus turned to the dynamics of magnetic dipoles orbiting a static BH in the SBR gravity within an external uniform magnetic field. We observed that the behavior of the effective potential and angular momentum of the magnetic dipole similar to that of a charged test particle. However, the dependence of the ISCO radius on the magnetic interaction parameter α was different. It was demonstrated that with an increase in α, the ISCO radius could exponentially rise, starting from $\alpha \sim 0.3$. The conventional impact of the parameter β on the ISCO radius was also evident. A degeneracy plot for the matching ISCO radii of magnetic dipoles in the spacetime of a BH in SBR gravity and in the Kerr spacetime revealed that the magnetic interaction parameter α could effectively replicate the effect of the spin of the Kerr BH, particularly for retrograde motion of the magnetic dipole. The influence of the parameter β on this phenomenon remained negligibly small.

In Section V, we have applied the outcomes of this study to the case when neutron star is assumed to behave as a magnetic dipole moving around the supermassive BH Sgr $A^\star$. We have shown that the coupling parameter α for such scenarios can be taken on the order of $\alpha \sim 10^{-1}$. Using such order of magnetic coupling parameter we have investigated how the magnetic field and the SBR gravity parameter β affect the orbits of neutron stars orbiting the supermassive BH. We have seen that an increase in α increases the ISCO radius, while an increase in β negligibly decreases it. Assuming that the rotating Kerr BH and a static BH in the SBR gravity immersed in an external uniform magnetic field can produce the same ISCO radii, we have obtained degeneracy plots between the spin of the Kerr BH and parameters involved in the spacetime solution selected in this study. It is observed that the magnetic coupling parameter can completely mimic the gravitational effect of the spin parameter for retrograde motion, while the β parameter can negligibly mimic the spin.

In all the scenarios presented in this study, we observed that the impact of the parameter β is most pronounced in the immediate vicinity of the BH. As one moves farther from the central BH, this effect diminishes considerably. We attribute this attenuation to several factors. Firstly, the spacetime solution provided is derived under the linear approximation of β, and higher-order terms may become significant for a comprehensive analysis. Secondly, the need to adhere to small values of β, stemming from the linear approximation, curtails the inherent characteristics of the SBR gravity. Consequently, this work serves as an initial exploration into understanding the properties of the SBR gravity, and broader investigations are imperative for a more comprehensive comprehension of this gravitational theory.

Data Availability Statement Data will be made available on reasonable request. [Author's comment: No new datasets are generated in this study.]

Code Availability Statement Code/software will be made available on reasonable request. [Author's comment: No new code/software is generated in this study.]

Funded by SCOAP[3].

References

1. K. Akiyama et al. (Event Horizon Telescope), Astrophys. J. Lett. **875**, L1 (2019). https://doi.org/10.3847/2041-8213/ab0ec7. arXiv:1906.1123 [astro-ph.GA]
2. K. Akiyama et al. (Event Horizon Telescope), Astrophys. J. Lett. **875**, L5 (2019). https://doi.org/10.3847/2041-8213/ab0f43. arXiv:1906.11242 [astro-ph.GA]
3. B.P. Abbott, R. Abbott, T.D. Abbott, M.R. Abernathy, F. Acernese, K. Ackley, C. Adams, T. Adams, (LIGO Scientific Collaboration and Virgo Collaboration), Phys. Rev. Lett. **116**, 061102 (2016). https://doi.org/10.1103/PhysRevLett.116.061102
4. K. Akiyama et al., Astrophys. J. Lett. **875**, L1 (2019). https://doi.org/10.3847/2041-8213/ab0ec7
5. S. Shankaranarayanan, J.P. Johnson, Gen. Relativ. Gravit. **54**, 44 (2022). https://doi.org/10.1007/s10714-022-02927-2. arXiv:2204.06533 [gr-qc]
6. S.V. Ketov, Universe (2022). https://doi.org/10.3390/universe8070351
7. R. Campos Delgado, S.V. Ketov, Phys. Lett. B **838**, 137690 (2023). https://doi.org/10.1016/j.physletb.2023.137690. arXiv:2209.01574 [gr-qc]
8. L. Rezzolla, B.J. Ahmedov, J.C. Miller, Mon. Not. R. Astron. Soc. **322**, 723 (2001). https://doi.org/10.1046/j.1365-8711.2001.04161.x. arXiv:astro-ph/0011316
9. L. Rezzolla, B.J. Ahmedov, J.C. Miller, Found. Phys. **31**, 1051 (2001). https://doi.org/10.1023/A:1017574223222. arXiv:gr-qc/0108057
10. B.V. Turimov, B.J. Ahmedov, A.A. Hakimov, Phys. Rev. D **96**, 104001 (2017). https://doi.org/10.1103/PhysRevD.96.104001
11. C.W. Misner, K.S. Thorne, J.A. Wheeler, *Gravitation* (W. H. Freeman, San Francisco, 1973)
12. R.M. Wald, Phys. Rev. D **10**, 1680 (1974). https://doi.org/10.1103/PhysRevD.10.1680
13. B. Narzilloev, J. Rayimbaev, S. Shaymatov, A. Abdujabbarov, B. Ahmedov, C. Bambi, Phys. Rev. D **102**, 104062 (2020). https://doi.org/10.1103/PhysRevD.102.104062. arXiv:2011.06148 [gr-qc]
14. S. Chen, M. Wang, J. Jing, JHEP **09**, 082 (2016). https://doi.org/10.1007/JHEP09(2016)082. arXiv:1604.02785 [gr-qc]
15. K. Hashimoto, N. Tanahashi, Phys. Rev. D **95**, 024007 (2017). https://doi.org/10.1103/PhysRevD.95.024007. arXiv:1610.06070 [hep-th]
16. S. Dalui, B.R. Majhi, P. Mishra, Phys. Lett. B **788**, 486 (2019). https://doi.org/10.1016/j.physletb.2018.11.050. arXiv:1803.06527 [gr-qc]
17. W. Han, Gen. Relativ. Gravit. **40**, 1831 (2008). https://doi.org/10.1007/s10714-007-0598-9. arXiv:1006.2229 [gr-qc]
18. A.P.S. de Moura, P.S. Letelier, Phys. Rev. E **61**, 6506 (2000). https://doi.org/10.1103/PhysRevE.61.6506. arXiv:chao-dyn/9910035
19. V.S. Morozova, L. Rezzolla, B.J. Ahmedov, Phys. Rev. D **89**, 104030 (2014). https://doi.org/10.1103/PhysRevD.89.104030. arXiv:1310.3575 [gr-qc]
20. A. Jawad, F. Ali, M. Jamil, U. Debnath, Commun. Theor. Phys. **66**, 509 (2016). https://doi.org/10.1088/0253-6102/66/5/509. arXiv:1610.07411 [gr-qc]
21. S. Hussain, M. Jamil, Phys. Rev. D **92**, 043008 (2015). https://doi.org/10.1103/PhysRevD.92.043008. arXiv:1508.02123 [gr-qc]
22. M. Jamil, S. Hussain, B. Majeed, Eur. Phys. J. C **75**, 24 (2015). https://doi.org/10.1140/epjc/s10052-014-3230-7. arXiv:1404.7123 [gr-qc]
23. G.Z. Babar, M. Jamil, Y.-K. Lim, Int. J. Mod. Phys. D **25**, 1650024 (2015). https://doi.org/10.1142/S0218271816500243. arXiv:1504.00072 [gr-qc]
24. M. Banados, J. Silk, S.M. West, Phys. Rev. Lett. **103**, 111102 (2009). https://doi.org/10.1103/PhysRevLett.103.111102. arXiv:0909.0169 [hep-ph]
25. B. Majeed, M. Jamil, Int. J. Mod. Phys. D **26**, 1741017 (2017). https://doi.org/10.1142/S0218271817410176. arXiv:1705.04167 [gr-qc]
26. A. Zakria, M. Jamil, JHEP **05**, 147 (2015). https://doi.org/10.1007/JHEP05(2015)147. arXiv:1501.06306 [gr-qc]
27. I. Brevik, M. Jamil, Int. J. Geom. Methods Mod. Phys. **16**, 1950030 (2019). https://doi.org/10.1142/S0219887819500300. arXiv:1901.00002 [gr-qc]
28. M. De Laurentis, Z. Younsi, O. Porth, Y. Mizuno, L. Rezzolla, Phys. Rev. D **97**, 104024 (2018). https://doi.org/10.1103/PhysRevD.97.104024. arXiv:1712.00265 [gr-qc]
29. S.R. Shaymatov, B.J. Ahmedov, A.A. Abdujabbarov, Phys. Rev. D **88**, 024016 (2013). https://doi.org/10.1103/PhysRevD.88.024016
30. B. Narzilloev, J. Rayimbaev, S. Shaymatov, A. Abdujabbarov, B. Ahmedov, C. Bambi, Phys. Rev. D **102**, 044013 (2020). https://doi.org/10.1103/PhysRevD.102.044013. arXiv:2007.12462 [gr-qc]
31. J.C. McKinney, A. Tchekhovskoy, R.D. Blandford, Mon. Not. R. Astron. Soc. **423**, 3083 (2012). https://doi.org/10.1111/j.1365-2966.2012.21074.x. arXiv:1201.4163 [astro-ph.HE]
32. J.M. Bardeen, W.H. Press, S.A. Teukolsky, Astrophys. J. **178**, 347 (1972). https://doi.org/10.1086/151796
33. A. Hakimov, A. Abdujabbarov, B. Narzilloev, Int. J. Mod. Phys. A **32**, 1750116 (2017). https://doi.org/10.1142/S0217751X17501160
34. J. Rayimbaev, B. Narzilloev, A. Abdujabbarov, B. Ahmedov, Galaxies (2021). https://doi.org/10.3390/galaxies9040071
35. B. Narzilloev, J. Rayimbaev, A. Abdujabbarov, B. Ahmedov, Galaxies (2021). https://doi.org/10.3390/galaxies9030063
36. B. Narzilloev, B. Ahmedov, Symmetry (2022). https://doi.org/10.3390/sym14091765
37. B. Narzilloev, B. Ahmedov, Symmetry **15**, 293 (2023). https://doi.org/10.3390/sym15020293
38. B. Narzilloev, A. Abdujabbarov, A. Hakimov, Int. J. Mod. Phys. A **37**, 2250144 (2022). https://doi.org/10.1142/S0217751X22501445
39. T. Mirzaev, S. Li, B. Narzilloev, I. Hussain, A. Abdujabbarov, B. Ahmedov, Eur. Phys. J. Plus **138**, 47 (2023). https://doi.org/10.1140/epjp/s13360-022-03632-4
40. B. Narzilloev, B. Ahmedov, Int. J. Mod. Phys. A **38**, 2350026 (2023). https://doi.org/10.1142/S0217751X23500264
41. F. Abdulxamidov, C.A. Benavides-Gallego, B. Narzilloev, I. Hussain, A. Abdujabbarov, B. Ahmedov, H. Xu, Eur. Phys. J. Plus **138**, 635 (2023). https://doi.org/10.1140/epjp/s13360-023-04283-9
42. H. Alibekov, B. Narzilloev, A. Abdujabbarov, B. Ahmedov, Symmetry (2023). https://doi.org/10.3390/sym15071414
43. A. Davlataliev, B. Narzilloev, I. Hussain, A. Abdujabbarov, B. Ahmedov, Phys. Dark Univ. **42**, 101340 (2023). https://doi.org/10.1016/j.dark.2023.101340
44. M. Alloqulov, B. Narzilloev, I. Hussain, A. Abdujabbarov, B. Ahmedov, Chin. J. Phys. **85**, 302 (2023). https://doi.org/10.1016/j.cjph.2023.07.005
45. B. Narzilloev, B. Ahmedov, Int. J. Mod. Phys. D **32**, 2350064 (2023). https://doi.org/10.1142/S0218271823500645

46. B. Narzilloev, A. Abdujabbarov, B. Ahmedov, C. Bambi, Phys. Rev. D **108**, 103013 (2023). https://doi.org/10.1103/PhysRevD.108.103013
47. S.V. Ketov, Universe **8**, 351 (2022). https://doi.org/10.3390/universe8070351. arXiv:2205.13172 [gr-qc]
48. E. Witten, Nucl. Phys. B **500**, 3 (1997). https://doi.org/10.1016/S0550-3213(97)00416-1. arXiv:hep-th/9703166
49. B. Narzilloev, A. Abdujabbarov, C. Bambi, B. Ahmedov, Phys. Rev. D **99**, 104009 (2019). https://doi.org/10.1103/PhysRevD.99.104009. arXiv:1902.03414 [gr-qc]
50. M. Kološ, Z. Stuchlík, A. Tursunov, Class. Quantum Gravity **32**, 165009 (2015). https://doi.org/10.1088/0264-9381/32/16/165009. arXiv:1506.06799 [gr-qc]
51. A. Tursunov, Z. Stuchlík, M. Kološ, N. Dadhich, B. Ahmedov, Astrophys. J. **895**, 14 (2020). https://doi.org/10.3847/1538-4357/ab8ae9. arXiv:2004.07907 [astro-ph.HE]
52. O. Kopáček, V. Karas, J. Kovář, Z. Stuchlík, Astrophys. J. **722**, 1240 (2010). https://doi.org/10.1088/0004-637X/722/2/1240. arXiv:1008.4650 [astro-ph.HE]
53. O. Kopáček, V. Karas, Astrophys. J. **787**, 117 (2014). https://doi.org/10.1088/0004-637X/787/2/117. arXiv:1404.5495 [astro-ph.HE]
54. D. Li, X. Wu, Eur. Phys. J. Plus **134**, 96 (2019). https://doi.org/10.1140/epjp/i2019-12502-9. arXiv:1803.02119 [gr-qc]
55. K. Akiyama, A. Alberdi, W. Alef, K. Asada, R. Azulay, A.-K. Baczko, D. Ball, M. Baloković, J. Barrett, D. Bintley et al., Astrophys. J. Lett. **875**, L5 (2019)
56. B. Narzilloev, J. Rayimbaev, A. Abdujabbarov, C. Bambi, Eur. Phys. J. C **80**, 1074 (2020). https://doi.org/10.1140/epjc/s10052-020-08623-2. arXiv:2005.04752 [gr-qc]
57. K. Mori, E.V. Gotthelf, S. Zhang, H. An, F.K. Baganoff, N.M. Barrière, A.M. Beloborodov, S.E. Boggs, F.E. Christensen, W.W. Craig, F. Dufour, B.W. Grefenstette, C.J. Hailey, F.A. Harrison, J. Hong, V.M. Kaspi, J.A. Kennea, K.K. Madsen, C.B. Markwardt, M. Nynka, D. Stern, J.A. Tomsick, W.W. Zhang, Astron. J. Lett. **770**, L23 (2013). https://doi.org/10.1088/2041-8205/770/2/L23. arXiv:1305.1945 [astro-ph.HE]